

# Electrochemical Impedance Spectroscopy of Bis-[Triethoxysilylpropyl]Tetrasulfide on Al 2024-T3 Substrates

W.J. van Ooij\* and D. Zhu\*\*

## ABSTRACT

Thin films of the hydrolyzed silane bis-[triethoxysilylpropyl]-tetrasulfide (sulfane) were deposited on alkaline-cleaned Al 2024-T3 panels and investigated by electrochemical impedance spectroscopy (EIS) using the noncorrosive electrolyte 0.5 M potassium sulfate ( $K_2SO_4$ ) aqueous solution. The effects of continuously immersing the films in this electrolyte and curing the films at room temperature or at 100°C in air were studied. Three equivalent circuits were proposed that fit the experimental data very well. A continuous increase of impedance and the appearance of an additional time constant with respect to time in EIS spectra during immersion, curing, and aging processes were explained by the hydrolysis of the ester groups to silanol groups and condensation of the latter to siloxane bonds in the film, and by the formation of an unknown interfacial phase between the cross-linked silane film and the aluminum oxide ( $Al_2O_3$ ). Reflection absorption Fourier transform infrared spectroscopy (RAIR) was used to enhance the interpretation of the EIS results. It was concluded that EIS in a noncorrosive electrolyte is a useful method for studying the stability of silane films formed on metals and can contribute to determining the optimum conditions for depositing silane films on metals for corrosion protection. The results of potentiodynamic polarization tests and salt spray testing (ASTM B117) confirmed the conclusion drawn from EIS that a fully cured sulfane-silane film provides excellent corrosion protection on Al 2024-T3.

Submitted for publication May 2000; in revised form, November 2000.

\* Department of Materials Science and Engineering, University of Cincinnati, Cincinnati, OH 45221-0012. E-mail: wvanooij@uceng.uc.edu.

\*\* Department of Materials Science and Engineering, University of Cincinnati, Cincinnati, OH 45221-0012.

**KEY WORDS:** Al 2024, aluminum, coatings, electrochemical impedance spectroscopy, film, Fourier transform infrared spectroscopy, salt spray testing, silanes

## INTRODUCTION

Surface treatment of metals by silanes of the type  $Y-CH_2CH_2CH_2-Si(OX)_3$  (where Y is an organo-functional group and X is a methyl or ethyl group) has attracted the attention of many industries in the past several years since it has become apparent that these treatments can be used for corrosion prevention, in addition to providing improved paint adhesion. Silane treatment has some inherent advantages over conventional treatments such as chromating and phosphating. These advantages include environmental compliance, simple application process, and outstanding corrosion protection of a wide range of metals and alloys.<sup>1-3</sup>

Thin silane films on metals are normally obtained by dipping the metals into dilute hydrolyzed silane solutions for a short time, followed by drying in air. The film thickness thus obtained is only around several hundreds of nanometers or less (i.e., considerably thinner than conventional conversion processes). Nevertheless, the metals can be protected very efficiently against various forms of corrosion.<sup>4-7</sup>

The mechanism of interaction between metals and silane molecules—when used as coupling agents—has been studied extensively.<sup>8-9</sup> These studies have suggested that silane films connect to metal substrates by forming strong covalent bonds with

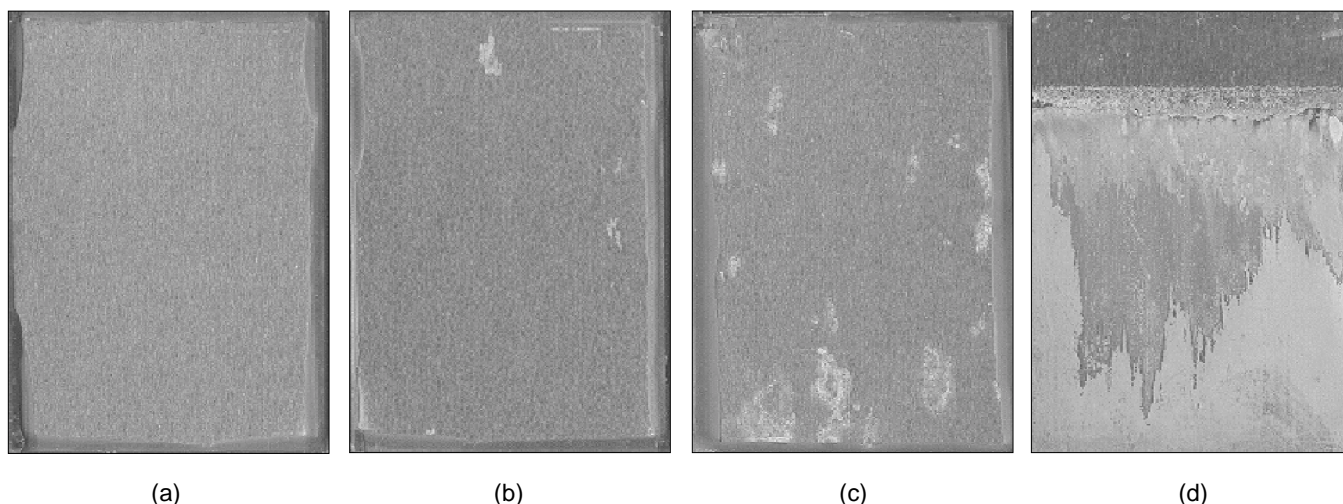


**FIGURE 1.** Alkaline-cleaned and silane-treated 7 cm by 10 cm Al 2024-T3 panels after 10-day immersion in naturally aerated 3.5% NaCl solution; the BTESPT silane films were deposited from a 5% solution in 95/5 ethanol/water by dipping for 30 s followed by blow drying; (a) film cured for 17 h at 100°C in air, (b) cured for 10 min at 100°C, (c) cured in ambient conditions for 24 h, and (d) alkaline-cleaned only. The blank panel was exposed vertically, and the others were exposed horizontally (i.e., completely immersed).

metals, such as Al-O-Si. However, in many cases, such bonds have remained elusive and have often been assumed but not actually demonstrated. In recent work, some evidence has been found that bis-type silanes can form reaction products with metals, such as sulfides, which may be formed when S-containing silanes are deposited on metals such as Zn, Cu, or Ni (i.e., with a high affinity for S).<sup>7</sup>

Van Ooij and coworkers have studied the corrosion protection performance of a variety of silane films on different metal substrates for several years.<sup>1-7</sup> They have demonstrated that silanes such as UPS,<sup>(1)</sup> VS,<sup>(2)</sup> and BTSE<sup>(3)</sup> can be used as effective anticorrosion agents if applied under appropriate process conditions, including proper concentration and pH of the silane solution and proper metal cleaning protocol. Recently, the focus of the research in this group has shifted to the anticorrosion behavior of some bis-type silanes, such as BTESPT<sup>(4)</sup> (sulfane) and bis-aminosilanes, since these silanes have been shown a wider application range than the previous ones. These silanes could thus be termed “universal silanes” because they cover more metals than UPS or BTSE, for instance. In the evaluation of the anticorrosion behavior of the sulfane, for example, BTESPT has been tested with good results on Al alloys, hot-dip galvanized (HDG) steel, electrogalvanized steel (EGS), Zn-Ni-coated steel, Galvannealed steel and

Galvalume<sup>†</sup>. The treated metals were tested in several tests, such as ASTM B117, ASTM D60-95, and ASTM D1654-92.<sup>11</sup> The results showed that the metals treated with the sulfane, by itself or mixed with a bis-aminosilane, survived these tests very well. Figure 1 shows a typical example of corrosion protection of Alloy Al 2024-T3 afforded by a BTESPT film during salt water immersion. The panel with the fully cured film (Figure 1[a]) was virtually free of any corrosion, whereas those that were not fully cured (Figure 1[b] and 1[c]) showed some signs of corrosion after 10 days.

Despite these excellent results, few understand the anticorrosion mechanism of the sulfane. Detailed information is also lacking on the optimum conditions for the application of BTESPT or other silanes that would give maximum protection. As Figure 1 shows, a high level of protection of the important aerospace alloy Al 2024-T3 was obtained after 17 h of curing the silane film at 100°C. However, such curing conditions would be unacceptable in industry. To reduce the severity of these curing conditions while maintaining the corrosion protection level shown in Figure 1, the effects occurring in the film during curing must be understood and measured. We have, therefore, started a program to unravel these mechanisms in more detail with particular emphasis on electrochemical impedance spectroscopy (EIS). The first results of these studies are presented in this paper. In addition to corrosion protection, the sulfane also has outstanding capabilities for bonding metals to a wide range of paints. The mechanism of this effect is not known either and is the subject of further studies. However, this paper concentrates on the cor-

<sup>(1)</sup> Ureidopropyltrialkoxysilane.

<sup>(2)</sup> Vinyltri(m)ethoxysilane.

<sup>(3)</sup> Bis-1,2-[triethoxysilyl]ethane.

<sup>(4)</sup> bis-[triethoxysilylpropyl]tetrasulfide (sulfane),  $(C_2H_5O)_3Si-(CH_2)_3-S_x-(CH_2)_3-Si(OC_2H_5)_3$  in which x has an average value of 3.8.<sup>10</sup>

<sup>†</sup> Trade name.

rosion inhibitory action of this silane in the absence of paint coatings.

EIS has been known for many years as a powerful tool in the corrosion research of metals coated with organic films, such as paints. Mansfeld, et al., and others have pioneered this technique.<sup>12-16</sup> Most of the initial work emphasized the use of EIS for continuous monitoring of the degradation process in coated metal systems in a corrosive environment such as 0.5 M sodium chloride (NaCl) solution. The technique can also be used to study the properties of the coating-metal interface rather than the coating degradation.<sup>17-18</sup> Only a few authors have characterized properties of an organic-coated metal system other than corrosion inhibition using a noncorrosive electrolyte.<sup>19</sup>

In this work, EIS measurements in 0.5 M potassium sulfate ( $K_2SO_4$ ) solution are reported for the BTESPT-coated Alloy Al 2024-T3. This electrolyte is noncorrosive but highly conductive (Appendix A). The sulfane provides excellent corrosion protection of this metal when immersed in salt solutions and also in the ASTM B117 test.<sup>3</sup> However, the degree of protection depends on the method of film deposition, such as its aging or curing conditions, solution pH, silane concentration, etc.  $K_2SO_4$  was used as an electrolyte in anticipation that concurrent corrosion reactions could be avoided, so that only data on the evolution of the sulfane film structure with time or process parameters on Al 2024-T3 would be obtained and analyzed.

Alloy Al 2024-T3, which is used extensively in aerospace, was chosen as the substrate since there is a great need to replace this alloy's current surface treatment by chromates with a more environmentally acceptable one. The silane studied here has been shown to be capable of completely protecting the alloy, even without paint coating, for 168 h or longer in the ASTM B117 salt spray test (SST). However, this level of protection is somewhat variable and not always reproducible. Apparently, some factors that contribute to the corrosion inhibitory performance of the silane film are not well known.

Thus, the objectives of the present work were to understand the evolution of the structure of the sulfane-silane film with time or process parameters on Al 2024-T3 substrates, to demonstrate that EIS can be used to characterize properties other than corrosion inhibitory performance of organic-coated metal systems, and to investigate whether EIS can be used to determine the optimum deposition conditions of this and other silanes.

## EXPERIMENTAL PROCEDURES

Bis-(3-triethoxysilylpropyl)tetrasulfide (sulfane) ( $[C_2H_5O]_3Si[CH_2]_3S_4[CH_2]_3Si[OC_2H_5]_3$ ) silane was provided by Witco Co. According to the manufacturer,

this silane contains bis-(3-triethoxysilylpropyl)tetrasulfane (< 50%), related silane esters with different S chain lengths (> 50%), and ethanol (< 0.1%). The average value of the S chain length is ~ 4, but actually ranges from 1 to 10.

Alloy Al 2024-T3 was purchased from ACT Laboratories, Inc. The panel dimensions were 10 cm by 15 cm and 1 mm thick. All panels were ultrasonically degreased with ethanol and acetone, alkaline-cleaned at 65°C with AC1055<sup>†</sup> cleaner (pH = 9) from Brent America, Inc. and rinsed with deionized (DI) water until the panel surface became water-break-free.

After cleaning, the Al 2024-T3 panels were immersed in a 5 vol% sulfane solution (silane/DI water/ethanol = 5/5/90 by vol%) at its natural pH of 6 for ~ 30 s. The treated panels were then removed from the solution and dried by blowing filtered air or curing at 100°C in air for a certain time. It should be noted that the 5 vol% sulfane solution was stabilized for at least 4 days before applying it to the metal since, in previous work, the solution did not attain its equilibrium state until 4 days after mixing.<sup>20</sup> The average silane film thickness after drying was found to be 350 nm, as determined by spectroscopic ellipsometry.<sup>21</sup>

Two process parameters, curing time and aging time, have been found to have significant influences on the structure and the performance of the sulfane-silane film on Al 2024-T3. To clarify the effects, two series of tests were conducted: To investigate the effect of curing time, sulfane-treated panels were cured at 80°C for various times ranging from 0.16 h to 6 h, and the panels were measured with EIS afterward. To study the effect of aging time, the treated panels without precuring at higher temperatures were aged at room temperature (RT) for 24 h to 840 h and then tested with EIS. In a third type of experiment, the effect of continuous immersion in the electrolyte on the silane film structure was investigated. EIS measurements were carried out on the sulfane-treated Al 2024-T3 panel when continuously immersed in 0.5 M  $K_2SO_4$  solution for immersion times ranging from 0.16 h to 24 h. The panel was cured for 0.16 h at 80°C just prior to immersion in the electrolyte.

The EIS measurements were carried out using an SR810<sup>†</sup> frequency response analyzer connected to a Gamry CMS100<sup>†</sup> potentiostat. The measured frequency range was from  $10^{-3}$  Hz to  $10^5$  Hz, with an alternating current (AC) excitation amplitude of 10 mV. A saturated calomel electrode (SCE) was used as the reference electrode and coupled with a graphite counter electrode. The surface area exposed to the electrolyte was 3.14 cm<sup>2</sup>. The distance between the electrodes and the tested area was ~ 6 cm. Per decade, seven experimental points were collected during the measurement around the open-circuit potential (OCP) of the treated system (-0.70 V to

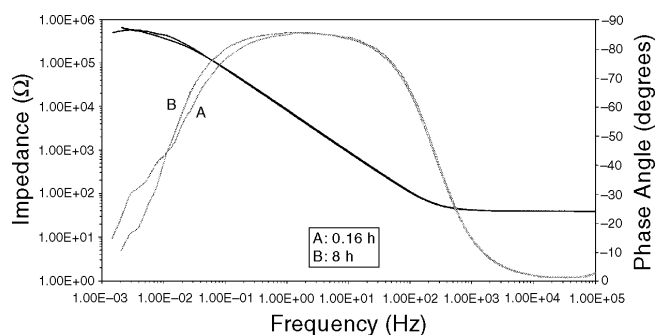


**FIGURE 2.** Bode plots for bare Al 2024-T3 during immersion in 0.5 M  $K_2SO_4$  solution for 0.16 h to 8 h.

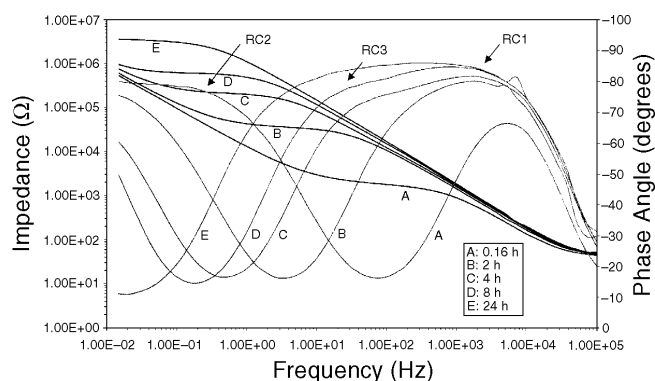


**FIGURE 3.** Bode plots for sulfane-treated Al 2024-T3 panels during immersion in 0.5 M  $K_2SO_4$  solution for 0.16 h to 24 h.

-0.55 V). A 0.5-M  $K_2SO_4$  solution was chosen as the electrolyte in this work for reasons outlined earlier. All EIS spectra were recorded after immersion in the electrolyte for ~ 10 min. The change in OCP was then < 0.01 V/s.

Reflection absorption Fourier transform infrared spectroscopy (RAIR) was used for surface analysis of sulfane-treated Al 2024-T3 in order to enhance the interpretation of EIS results. The absorption spectra were recorded on a Bio-Rad FTS-40<sup>†</sup> spectrophotometer with the IR range from 400  $cm^{-1}$  to 4,000  $cm^{-1}$ . All data shown in the paper were obtained with an incident angle of 75° perpendicular to the surface of the specimens, a spectral resolution of 4  $cm^{-1}$ , and a scan number of 200.

Potentiodynamic polarization tests were carried out at RT in 0.5 M NaCl (pH = 6) aqueous solution to compare the corrosion behavior of Al 2024-T3 with and without sulfane treatment. The panels with an exposure area of 0.78  $cm^2$  were immersed in the electrolyte for 40 min before testing to achieve a steady state. All data were recorded between a cathodic potential of -900 mV<sub>SCE</sub> and an anodic potential of 0 mV<sub>SCE</sub>, with a scanning rate of 1 mV/s. SCE was used as the reference electrode and Pt the counter electrode.

Sulfane-treated Al 2024-T3 panels were exposed to a SST (ASTM B117) for 360 h in the Harshaw salt spray chamber. Four replicates were prepared for each treatment. Chromated (treated by Chromi-coat 103<sup>†</sup>) and alkaline-cleaned Al 2024-T3 were chosen as controls. The corrosion evaluation after testing was made based on the standard method of "Evaluation of Corrosion Phenomena" provided by Chemetall/GmbH.

## RESULTS AND DISCUSSION

EIS data were collected for bare Al 2024-T3 panels during immersion in 0.5 M  $K_2SO_4$  solution for various times, as shown in Figure 2. The purpose of this experiment was to determine any changes in the natural aluminum oxide ( $Al_2O_3$ ) film when exposed to the noncorrosive 0.5 M  $K_2SO_4$  solution. As shown in Figure 2, only one time constant corresponding to the oxide film appears, and very little change occurred during 8 h of immersion. EIS measurements for bare Al 2024-T3 panels cured at 100°C for 0.16 h and 8 h were also done. Again, no significant differences were observed with curing time. Thus, the conclusion can be drawn that the natural  $Al_2O_3$  film remained stable during immersion and curing (100°C) processes. Any changes observed in the EIS spectra of the silane-coated Al 2024-T3 must be the result of specific interactions with or by the silane film.

### EIS Results for the Three Types of Experiments

*Effect of Immersion Time of Sulfane-Treated Al 2024-T3 in 0.5 M  $K_2SO_4$*  — Figure 3 shows the Bode plots for the sulfane-treated and cured (0.16 h at 80°C) Alloy Al 2024-T3 as a function of immersion time in the 0.5 M  $K_2SO_4$  solution. It can be seen that the total impedance of the system increased with immersion time throughout most of the measured frequency range, with the appearance of a distinctive additional time constant after 4 h of immersion. The additional time constant is shown more clearly in the phase angle plot than in the impedance plot.

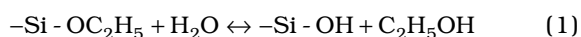
At the initial immersion stages (0.16 h to 2 h), only two time constants were observed, one (resistance-capacitance [RC]1) located at high frequencies (~ 10<sup>4</sup> Hz), and the other (RC2) at low frequencies (~ 0.1 Hz). Since the sulfane-silane film was coated uniformly on the Al 2024-T3 surface, these two time constants can most likely be assigned to the silane film (RC1) and the  $Al_2O_3$  (RC2).

As the immersion process continued (after 4 h of immersion), the impedance of the sulfane-silane film (RC1) increased remarkably, and, correspondingly, the time constant RC1 shifted to lower frequencies. Interestingly, an additional time constant (RC3) occurred in the phase angle diagram in the medium frequency range between RC1 and RC2. Also, the

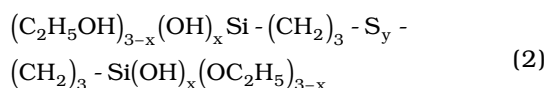
low-frequency impedance kept increasing even after 24 h of immersion (curve E in Figure 3), but instead of two distinctive time constants, only one broadened time constant appeared in the medium frequency range. This was probably a result of the overlap of the two time constants (RC3 and RC1).

In general, the observed increase in the total impedance and the appearance of an additional time constant may indicate the formation(s) of some new, highly water-resistant structure(s) in the sulfane-silane film and/or at the interface of the silane film and the Al<sub>2</sub>O<sub>3</sub> layer. A better understanding of these observations could shed more light on the mechanism of the silane film formation on metal substrates. Plausible mechanisms associated with the changes in EIS are discussed here.

*The Formation of Cross-linked Silane Film* — As is well-known, the formation of a cross-linked silane film containing siloxane bonds Si-O-Si is the result of the condensation/cross-linking of silanol groups -Si-OH, which are initially formed by the hydrolysis of ester groups (-Si-OC<sub>2</sub>H<sub>5</sub>) in the dilute water/alcohol silane solution.<sup>1,8</sup> In previous work, it was found by RAIR and Time-of-Flight Secondary Ion Mass Spectroscopy (ToFSIMS) analysis of sulfane films that this bis-silane cannot be hydrolyzed completely in the 5 vol% solution of natural pH 6. Therefore, some nonhydrolyzed ethoxy ester groups still remain in the applied silane film on the metal substrate.<sup>22</sup> This effect is a consequence, in part, of the low solubility of the silane ester in water. It can only be dissolved in 90/10 alcohol/water mixtures. This high alcohol content drives the hydrolysis equilibrium:



to the left, resulting in a film of the type:



rather than (OH)<sub>3</sub>-Si-(CH<sub>2</sub>)<sub>3</sub>-S<sub>y</sub>-(CH<sub>2</sub>)<sub>3</sub>-Si(OH)<sub>3</sub>, which would be obtained if the silane ester were water-soluble. Here, the subscript x is the number of hydrolyzed ester groups, and the subscript y the number of S atoms in the sulfane-silane molecule.

When this partially hydrolyzed silane film on Al 2024-T3 is immersed in the 0.5 M K<sub>2</sub>SO<sub>4</sub> aqueous solution for a certain time, these remaining ester groups in the silane film are likely to slowly hydrolyze further to generate silanol groups (Si-OH) and such silanol groups to condense or cross-link to form siloxane-containing structures in the existing film. As a result, the amount of the siloxane units in the film increases slowly during immersion. It is known that in pure water condensation of silanol groups always occurs slowly (i.e., the large amount of water

present does not drive the condensation reaction to the left).<sup>8</sup> Acid or base catalyzes this condensation strongly, but in the experiments the pH of the electrolyte was ~ 6. It is also known that siloxane structures are fairly resistant to hydrolysis by water, at least at RT. A conclusion thus can be drawn that the further formation of siloxane-like structures in the partially hydrolyzed sulfane-silane film is likely to be one of the major causes of the increase of the total impedance (Figure 3). This also implies that EIS can measure these hydrolysis and condensation effects quantitatively.

There is an analogy here with solid-state dielectric spectroscopy where state-of-cure of resins is measured by recording the impedance of the polymer using a two-electrode system.<sup>23</sup> In this study, however, the traditional three-electrode approach was used with the sulfane-silane film fully immersed in electrolyte. This allowed comparing the EIS response with that obtained from a corrosive electrolyte (e.g., NaCl) where the protective properties of the silanes could be evaluated.

It should now be clear why the sulfane-silane film was precured at moderate conditions prior to immersion in the electrolyte. This step condensed most of the free silanol groups present in the film as a result of the hydrolysis reaction in the water/alcohol mixture of pH 6. Therefore, what can be observed in the EIS data is mainly the hydrolysis and condensation of the remaining ester groups in the film that were not hydrolyzed in the water/alcohol mixture. Also obvious is the advantage to performing EIS in the noncorrosive electrolyte since concurrent corrosion reactions resulting from the presence of Cl<sup>-</sup> ions would obscure the effects observed in Figure 3. The equivalent circuit would become too complex to extract the data on the silane cross-linking reliably.

It should also be pointed out that although the initial sulfane-silane films were not stable with respect to time, the curves were still smooth enough to be fitted with the equivalent circuit. The initial sulfane-silane films could be considered an open, non-barrier structures, as the lack of purely capacitive response can be seen in the EIS spectra (Curve A, Figure 3).

*The Formation of an Interfacial Phase* — Another contribution to an increase in the total impedance shown in Figure 3 might be the formation and growth of a new interfacial phase, corresponding to the additional time constant (RC3) shown in Figure 3. Presently, there is still lack of detailed knowledge on the chemistry of this phase, but the phase may be a product formed by a reaction between the sulfane-silane film and aluminum hydroxide [Al(OH)<sub>3</sub>] similar to that observed with other silanes in previous silane work.<sup>8,24</sup> In Reference 23, evidence by XPS and FTIR was presented for the formation of Al-siloxane compounds formed by condensation reactions between

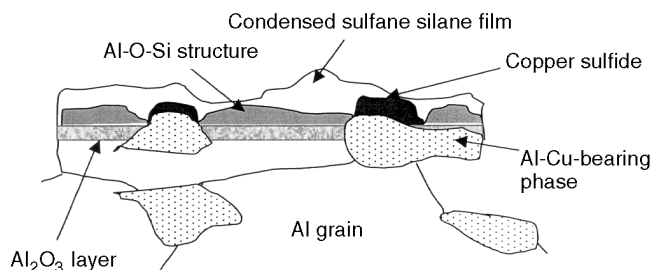


**FIGURE 4.** Schematic of a plausible interfacial structure between the sulfane-silane film and Alloy Al 2024-T3.

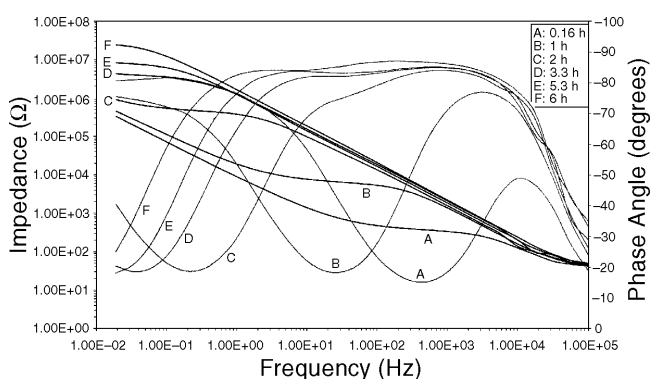
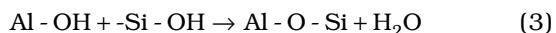


**FIGURE 5.** Bode plots for sulfane-treated Al 2024-T3 panels cured at 80°C in air for 10 min to 370 min, then tested by EIS in 0.5 M  $K_2SO_4$ .

silanol groups and  $Al_2O_3$  when 99.9% Al was treated with methacryloxypropyltrimethoxysilane. This polymeric passive film hinders ion diffusion; hence, improved general and localized corrosion of pure Al. Two plausible interfacial structures are Al-siloxane structures and sulfide compounds.

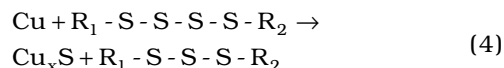
**Al-Siloxane Structure (Al-O-Si)** — The condensation reaction between  $Al(OH)_3$  and silanol groups in a sulfane-silane film is as follows:<sup>8</sup>



The resultant Al-siloxane bond, Al-O-Si, is known as a strong covalent bond that gives excellent adhesion of silane film to the Al substrate.<sup>8,24</sup> If the  $Al(OH)_3$  is porous, the silane can penetrate into and react with the layer and a three-dimensional structure containing these bonds is formed.

**Sulfide compounds ( $Cu_xS$ )** — As is well known, Alloy Al 2024-T3 contains a considerable amount of Al-Cu-bearing second phase particles throughout the Al matrix. These particles make the alloy sensitive to various forms of corrosion such as pitting and intergranular corrosion. Recent work with the sulfane-silane, on the other hand, has shown that sulfides can be formed from the reaction between the sulfane-silane film and metals such as Zn, Cu, and Ni with

high affinity for S.<sup>7</sup> The reaction of S in organic sulfides with Cu is:<sup>25</sup>



$Cu_xS$  is a non-stoichiometric copper sulfide. It is very likely that the Al-Cu-bearing phase will react with the sulfane-silane film in the same way.

Thus, a plausible interfacial structure between sulfane-silane and Al 2024-T3 may consist of two types of structures, as shown in Figure 4. The Al-O-Si structure is mainly formed between the sulfane-silane film and  $Al_2O_3$  layer while the  $Cu_xS$ -like compound may be located at the sites of the Al-Cu-bearing phase.

Further characterization work such as RAIR and ToFSIMS will be necessary to identify this new structure. The function and relevance of this new structure in the corrosion protection of silane-treated Al 2024-T3 will also be investigated using EIS in a corrosive electrolyte (e.g., 0.5 M NaCl).

**Effects of Curing Time at 80°C and Aging Time in Ambient Condition on Sulfane-Treated Al 2024-T3** — EIS behavior similar to that shown in Figure 3 was observed for the effect of the silane curing time (0.16 h to 6 h at 80°C in air) on sulfane-treated Alloy Al 2024-T3 (Figure 5), except that the changes in the spectra developed faster for the curing time effect than for the immersion time effect. The new time constant RC3 was also formed here. This result is in agreement with our interpretation of the effects of Figure 3, as during the thermal cure the film adsorbed sufficient atmospheric moisture for hydrolysis of the remaining ethoxy ester groups. The ethanol molecules evaporated immediately, driving the reaction to the right. The silanol groups condensed readily under these circumstances, and the water released in the condensation reaction was then available again for further hydrolysis. In other words, the effects during thermal cure were autocatalytic and the films cross-linked quickly, requiring only a small amount of atmospheric humidity.

The changes in the EIS spectra of the sulfane-treated Al 2024-T3 with aging time in air at ambient conditions are shown in Figure 6. After aging, each sample was immersed in the electrolyte and the EIS spectrum was recorded. The total impedance increased with aging time throughout the entire exposure period, with only two observed time constants corresponding to the sulfane-silane film (RC1) and the  $Al_2O_3$  layer (RC2), as in Figure 3. However, the additional time constant (RC3) indicative of a new interfacial phase formed in the immersion process was not observed during 120 h of aging. Apparently this phase can form during continuous immersion in electrolyte at RT, or during curing at 80°C, but not easily during short-term aging in ambient conditions. It was noted, however, that after 840 h of aging, the

low-frequency impedance had increased significantly, while one broadened time constant appeared in the phase angle diagram, which was probably a result of the overlap of the two time constants for the unknown phase and outer silane film. The tendency in Figure 6 indicates that the partly cross-linked film of the sulfane is moisture-sensitive and hydrolyzes and cross-links readily during storage at ambient conditions. The importance of this observation is that a more quantitative analysis of this effect would indicate how long a film should be stored and in what conditions before it should be exposed to a corrosive environment, assuming that the best corrosion protection will be obtained once the film is completely hydrolyzed and cross-linked. As stated before, films of hydrophobic silanes cannot easily be hydrolyzed fully to monomeric silanes, so the final hydrolysis followed by cross-linking has to be done on the deposited film. These “conditioning” effects could be accelerated by storing the films in high-humidity conditions.

**Dependence of Observed Effects on Type of Substrate** — The tests described above were repeated with sulfane-treated bright-annealed stainless steel panels of AISI Type 436. The EIS results showed behavior very similar to that on Al 2024-T3, except for the slow formation of the new time constant RC3. Thus, it can be concluded that the effects observed during immersion and curing are not dependent on the substrate but reflect the characteristics of this silane film itself. The RC3 time constant difference, however, indicates that the reactivity of the silane towards the substrate depends on the nature of the substrate, as can be expected.

### Analysis of the Fitted Data for Silane-Treated Al 2024-T3

**Equivalent Circuits for Sulfane-Treated Al 2024-T3** — Several configurations of equivalent circuits (EC) concerning sulfane-treated Al 2024-T3 were tested. Figures 7 and 8 show three general models and their possible corresponding physical structures for the sulfane-treated Al 2024-T3. These models were suggested primarily based on the information extracted from the phase angle plots, which gave more details on the evolution of the silane-treated system with time and more clearly indicated the presence of a new phase. Constant phase elements (CPE) instead of an ideal capacitor were used in these models because none of the films formed can be expected to be perfect capacitors. With CPE the fit was considerably better than with capacitances.

As Figure 7 shows, the data obtained for the earlier stages were fitted with an EC consisting of 2 time constant units (Figure 7[a]). At this stage, the sulfane-silane film was very porous and readily permeable to the electrolyte, as no significant structural change caused by hydrolysis and cross-linking inside was observed in EIS.

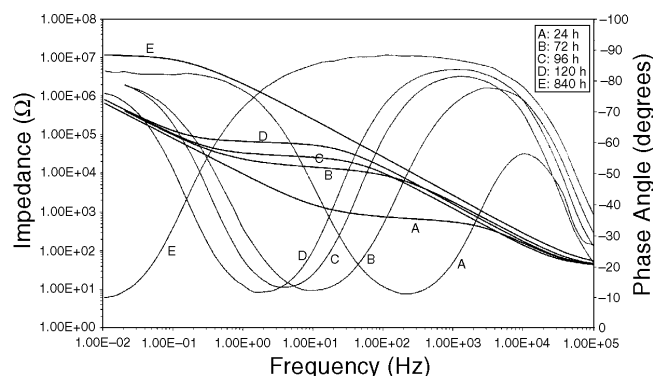


**FIGURE 6.** Bode plots for sulfane-treated Al 2024-T3 panels aged in air at RT and then tested by EIS in 0.5 M  $K_2SO_4$ .

At a later stage of the development of the film properties, when the new time constant had become apparent, a third RC element (“unknown phase”) was added (Figures 8[a] and 8[c]). The sulfane-silane film had become condensed and pores were being closed by the extensive cross-linking of silanol groups during this period. The film was less permeable to the electrolyte. Furthermore, the formation of the unknown phase improved the water resistance of the entire system. Figures 8(a) and 8(c) show two EC models suggested for EIS data fitting at the later stages. No significant difference can be found in the EIS fitted data between these two EC. Two possible structures corresponding to these two EC models are shown in Figures 8(b) and 8(d). The structure associated with the EC in Figure 8(a) consisted of a condensed sulfane-silane film at the topside, followed by an unknown phase layer covering uniformly the  $Al_2O_3$  layer (Figure 8[b]). The structure corresponding to the EC in Figure 8(c), however, demonstrates that the unknown phase may mix with the  $Al_2O_3$  layer to some extent. The determination of the exact structure of the system will be subjected to further characterization work instead of EIS.

Figures 9(a) through 9(d) show the fitted Bode plots representing the changes in EIS spectra of the sulfane-treated Al 2024-T3 with immersion time in 0.5 M  $K_2SO_4$  solution. An excellent agreement can be observed between the experimental data (points) and the fitted curve (solid line). Since the properties of the sulfane-treated Alloy Al 2024-T3 changed so rapidly with time, a deviation from ideal dielectric properties is possible (i.e., the sample may have changed during the time required to record the entire EIS spectrum). Therefore, CPE rather than capacitances was used in the models, which more accurately describes the dielectric properties in a non-ideal organic coated system. A CPE is usually defined as:<sup>26</sup>

$$Z(\text{CPE}) = \frac{(j\omega)^{-n}}{Y_0} \quad (5)$$

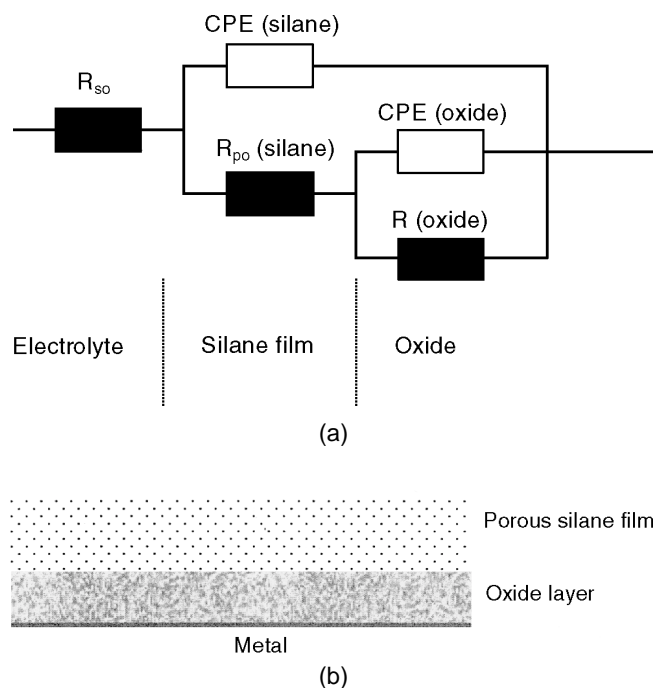


**FIGURE 7.** Equivalent circuits and their possible corresponding physical structures for sulfane-treated Al 2024-T3 at initial stages (without unknown phase): (a) EC and (b) the physical structure.

where  $Z$  is the impedance of the CPE in  $\Omega$ ,  $w$  is the angular frequency in rad/s,  $n$  and  $Y_0$  are the CPE parameters, and  $n$  is also the deviation from ideal behavior. For  $n = 1$ , the element is an ideal capacitor and  $Y_0$  is then equal to the capacitance,  $C$ . For  $n = 0$ , the CPE becomes a pure resistor with  $R = 1/Y_0$ . The capacitance can be calculated from the experimentally determined CPE parameters  $n$  and  $Y_0$  by the following equation:<sup>27-28</sup>

$$C = \frac{Y_0 \omega^{n-1}}{\text{Sin}\left(n \frac{\pi}{2}\right)} \quad (6)$$

In Figure 9(a), the fit for the sample immediately after immersion is slightly poorer than the EC in Figure 7(a). The two-time-constant circuit was preferred here since the phase angle plot did not indicate the presence of the time constant RC3 yet. The slight misfit in Figure 9(a) is most likely caused by a time factor. The EIS analysis took  $\approx 40$  min. In that time period, changes had already taken place in the film.

*Analysis of the Fitted Data for Sulfane-Treated Al 2024-T3* — Figure 10 shows resistance and capacitance as functions of immersion time of the sulfane-treated samples in the electrolyte. The capacitances were calculated from the fitted  $Y_0$  and  $n$  values using Equation (6). The figure also shows the values of  $n$ , which is a measure of the deviation from ideal capacitive behavior.

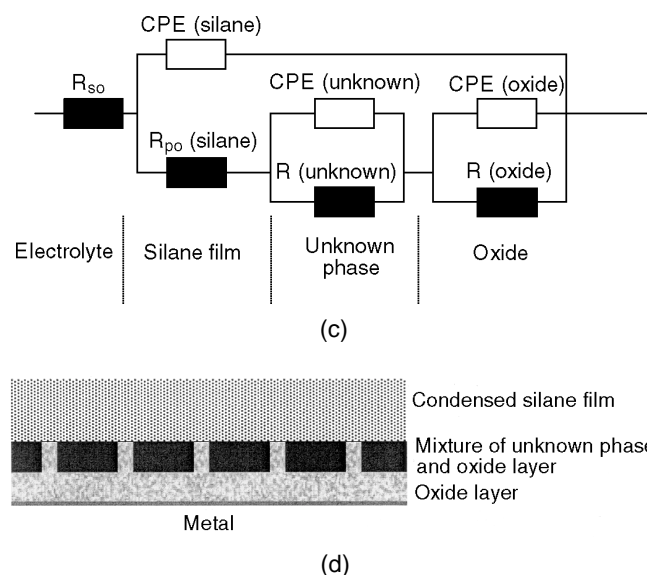
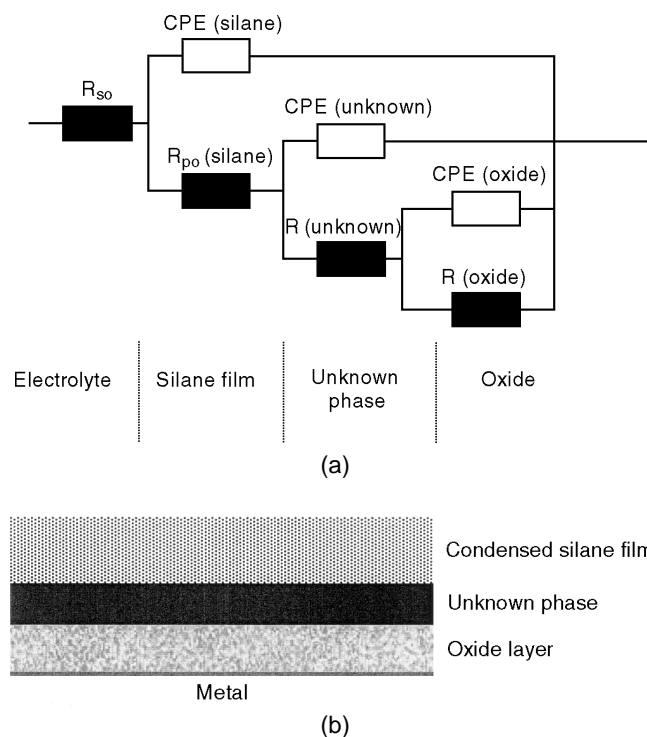


**FIGURE 8.** Equivalent circuits and their possible corresponding physical structures for sulfane-treated Al 2024-T3 at later stages (with unknown phase): (a) complete-nested EC, (b) the physical structure corresponding to (a), (c) half-serial EC, and (d) the physical structure corresponding to (c).

The values of the resistances for both the silane film and the unknown phase (starting after 2 h) increased with immersion time. A stationary situation was not reached during the measuring period; in other words, the formation of the siloxane structures in the silane film continued and the increased cross-linking led to a higher resistance. The resistance increase of the unknown phase may have resulted from

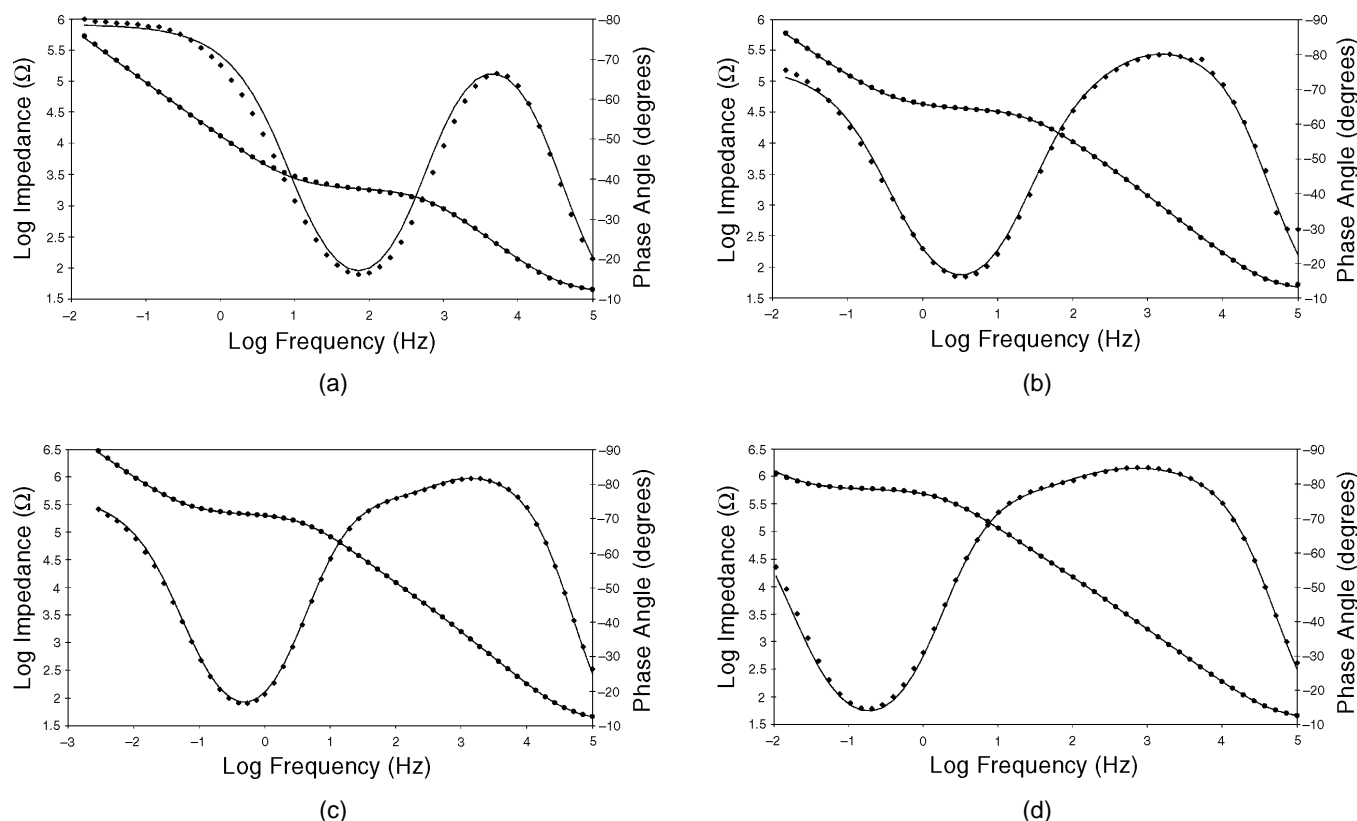


**FIGURE 9.** Fitted Bode plots for sulfane-treated Al 2024-T3 after immersion in 0.5 M  $K_2SO_4$  solution for various times: (a) 0.16 h, (b) 2 h, (c) 4 h, and (d) 8 h.

the growth of this film. On the other hand, the values of the capacitances for the sulfane-silane films and the unknown phase decreased with immersion time. This phenomenon is unusual for common organic coatings such as paints. The capacitance of a paint coating always tends to increase with immersion time, even in a noncorrosive electrolyte, as a result of water uptake.<sup>19</sup> The reason for the increase in capacitance of such coatings is a significant increase of the dielectric constant ( $\epsilon$ ) of the coating, which is influenced strongly by water penetration into the coating. This conclusion is valid if we assume that the coating thickness remains constant during water penetration since the capacitance of a coating can be defined as follows:<sup>27-28</sup>

$$C = \epsilon_0 \epsilon \frac{A}{d} \quad (7)$$

in which the parameters have their usual meanings:  $A$  = surface area,  $d$  = coating thickness, and  $\epsilon_0$  = dielectric constant of the free space;  $\epsilon$  and thickness  $d$  are usually considered the important factors for the change of capacitance.

In the case of the sulfane-treated Al 2024-T3 panels, the observed decrease of the capacitances vs immersion time could be explained as follows.

For the silane film the increase of the siloxane concentration (cross-link density) in the film was associated with a reduction of the swelling capacity of the film. This effect reduced the  $\epsilon$  of the sulfane-silane film since the water content became lower as the cross-link density increased. That is, the film became more hydrophobic or less polarizable as it cross-linked more and the number of hydrophilic  $-\text{Si}-\text{OH}$  groups diminished. Again, the water content decreased.

For the new phase, the decrease of capacitance can most likely be attributed to the increase of the film thickness (d) as the film kept growing with time, although it cannot be excluded that the  $\epsilon$  for the new phase may have been somewhat lower than that for the silane film.

The  $n$  values showed an interesting trend. For the silane film they started at 0.92 and then increased to 0.96, so the silane film appeared to be of good quality and became even better as it cured. The  $n$  of the new phase ( $n'$  in the figures) started considerably lower and then increased to 0.85. This observation suggests that the film may have initially formed heterogeneously at local patches and then gradually grew to a more homogeneous film.

Figures 11 and 12 show the change of the resistances, capacitances, and  $n$  values with time in the

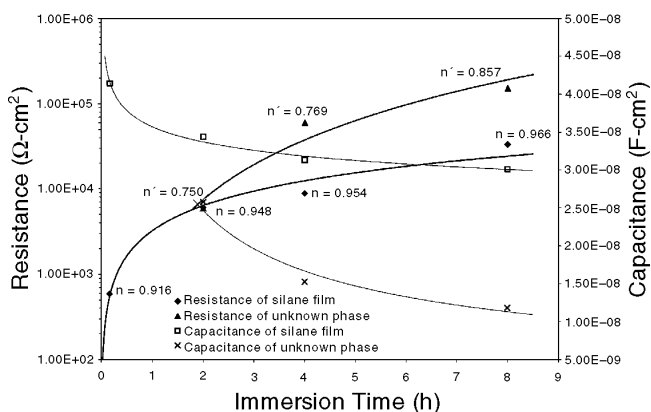


**FIGURE 10.** Capacitance and resistance as functions of immersion time in 0.5 M  $K_2SO_4$  solution for sulfane-treated Al 2024-T3;  $n$  and  $n'$  are for silane film and unknown phase, respectively.

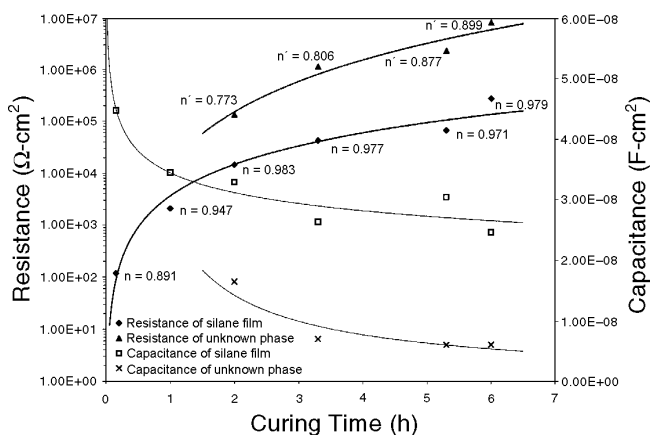


**FIGURE 11.** Capacitance and resistance as functions of curing time at 80°C for sulfane-treated Al 2024-T3;  $n$  and  $n'$  are for silane film and unknown phase, respectively.

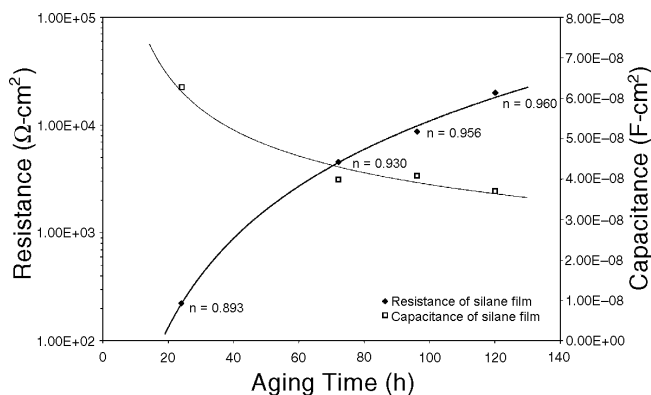


**FIGURE 12.** Capacitance and resistance as functions of RT aging time on Al 2024-T3 substrate.

sulfane-treated Al 2024-T3 samples observed in 80°C curing and the RT aging experiments, respectively. Behaviors similar to those in the immersion experiment are observed here, except that the progress in

the 80°C curing case (Figure 11) is much faster than in the immersion experiment. The values for the unknown phase could not be obtained in the RT aging experiment, since no new RC element was found (i.e., this unknown phase does not seem to be formed in this short-term and low-temperature aging process). The resistance values in the 80°C curing experiment are considerably higher than those observed in the short-term immersion RT aging experiments. Thus, the degree of cross-linking that can be attained in thermal aging at elevated temperature is higher than that observed in the other experiments. This in itself is not surprising, but it is remarkable to notice in Figure 11 that the silane film could not be fully cured even after 6 h of curing at 80°C because the resistance and capacitance of the silane film still tended to increase or decrease afterwards. However, higher temperatures can be expected to accelerate the curing process. In practice, it has been found that a fully cured silane film can be obtained by curing at 100°C for 4 h. This conclusion is of paramount importance for the successful and reproducible application of this silane for corrosion protection in the field. It explains why unpredictable and sometimes erratic behavior of the same silane-metal combination was observed previously, as hitherto there was no method available to determine the state of cure of the film. This state is determined not only by the curing temperature and time, but also by the relative humidity since the ester groups have to be removed by hydrolysis first.

The  $n$  values showed the same trends as in Figure 10: for the sulfane-silane film a slight increase with aging was observed. For the unknown phase (Figure 11 only), a steeper increase was found. The final values for both the silane film and the unknown phase are the same in all tests.

It should also be noted that the value of the resistance of the new phase between the silane film and the  $Al_2O_3$  layer was always of the same or higher order of magnitude as that of the silane film, while its capacitance was always lower. This is an important finding because it suggests that this unknown phase may provide a major contribution to the overall corrosion protection of the treated metal. Therefore, it is important to identify the composition and structure of this new phase so that its formation may be understood and its properties maximized in terms of corrosion protection. Future work will focus on this aspect.

The fitted EIS data for both the  $Al_2O_3$  layer and electrolyte are listed in Appendix B. The CPE parameter of the  $Al_2O_3$  layer,  $Y_0$ , decreased with time in all processes. This may indicate that the properties of the  $Al_2O_3$  layer had changed, though the causes are still unknown. Possibly, the properties could have been influenced by the reaction of Si-OH and  $Al(OH)_3$ . In addition, the dielectric constants of sulfane-silane

film in the curing process were calculated using Equation (7) to make an internal check for the validity of the EIS analysis (Appendix B, Table B4).

### Surface Analysis by RAIR Spectroscopy

Figure 13 compares the absorption spectra of sulfane-treated Al 2024-T3 aged in air at RT from 0 h to 72 h. The assignments of characteristic absorption bands for sulfane-silane film are given in Table 1.<sup>25,29-30</sup>

As can be seen in Figures 13(a) and 13(b), the intensities of the absorption bands corresponding to silanols (Si-OH) at 3,531, 3,363, 3,243 and 888  $\text{cm}^{-1}$  decreased with aging time while those corresponding to siloxane bonds (Si-O-Si) in the region of 1,176  $\text{cm}^{-1}$  to 1,000  $\text{cm}^{-1}$  increased during the aging period. This indicates the occurrence of further cross-linking in the sulfane-silane film. The band of Si-O-Si at 1,110  $\text{cm}^{-1}$  showed a 20  $\text{cm}^{-1}$  shift in the direction to high frequencies after 72 h of aging in air at RT. The shift may have been associated with the formation of linear siloxane chains during cross-linking.

The bands of CH stretching in unhydrolyzed ethoxy ester groups (Si-O-CH<sub>2</sub>CH<sub>3</sub>) at 2,972, 2,924, 2,886, and 951  $\text{cm}^{-1}$  decreased with time as a result of further hydrolysis of esters to silanols in the sulfane-silane film. The same effects could be observed during the immersion and curing processes with RAIR. Figures 14(a) and 14(b) present the spectra of sulfane-treated Al 2024-T3 immersed in 0.5 M K<sub>2</sub>SO<sub>4</sub> solution from 0 h to 20 h. The specimen was precured at 80°C for 10 min before immersion.

It is also interesting to note that the shoulders at 1,034  $\text{cm}^{-1}$  and 1,010  $\text{cm}^{-1}$  in Figures 13(b) and 14(b) continued to grow throughout immersion and aging. These shoulders may have been related to inorganic Al-O-Si bonds in the interfacial layer as suggested by EIS results. A similar observation of a Si-O-Al bond in the IR spectrum was also reported.<sup>24</sup> In general, RAIR analysis is in a good agreement with the EIS results and the interpretations presented in the earlier sections.

### Potentiodynamic Polarization Tests

The potentiodynamic polarization curves measured in 0.5 M NaCl solution at pH 6 for the Al 2024-T3 untreated and treated by sulfane-silane with and without curing (80°C for 20 h) are shown in Figure 15. Compared with these curves, it is obvious that both cathodic reduction reaction and anodic reaction on Al 2024-T3 were inhibited efficiently by the treatment with the sulfane-silane. Furthermore, the almost fully cross-linked sulfane-silane film (Curve A, 80°C, 20 h) provided even better corrosion protection on Al 2024-T3 than the porous silane film (Curve B, not cured). Again, the results of potentiodynamic polarization tests are consistent with the conclusion drawn from the EIS study (i.e., a fully cross-linked

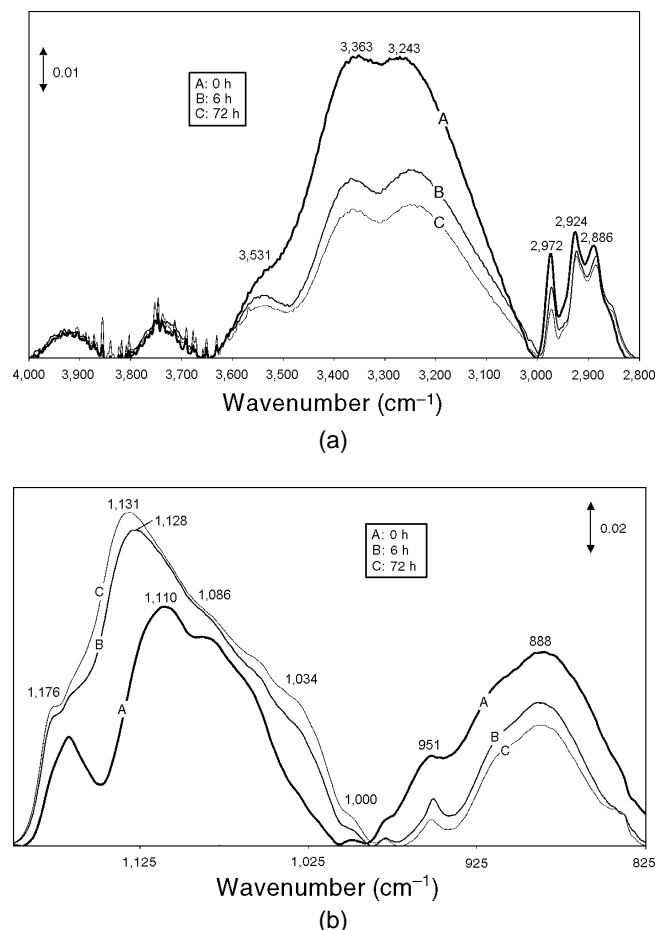


**FIGURE 13.** RAIR spectra of sulfane-treated Al 2024-T3 aged in air at RT from 0 h to 72 h: (a) 4,000  $\text{cm}^{-1}$  to 2,700  $\text{cm}^{-1}$  and (b) 1,200  $\text{cm}^{-1}$  to 825  $\text{cm}^{-1}$ .

**TABLE 1**  
Assignments of Characteristic Absorption Bands for Sulfane-Silane Film on Al 2024-T3

Absorption Band ( $\text{cm}^{-1}$ )	Assignment
3,531, 3,363, 3,243	Si-OH (H-bonded)
2,972, 2,924, 2,886	Si-O-CH <sub>2</sub> CH <sub>3</sub> (C-H)
1,176 to ~ 1,000	Si-O-Si, Si-O-C, and Si-O-Al region
951	Si-O-CH <sub>2</sub> CH <sub>3</sub> (Si-O-C)
888	Si-OH

structure with a high impedance in EIS spectrum provided an appreciable reduction in both cathodic and anodic currents in potentiodynamic polarization tests).

### SST (ASTM B117)

A SST was designed for comparing the corrosion behavior of Al 2024-T3 untreated and treated by sulfane-silane and by chromate. In order to obtain a fully cross-linked structure, sulfane-treated Al 2024-T3 was cured at 100°C for 10 min and then aged in

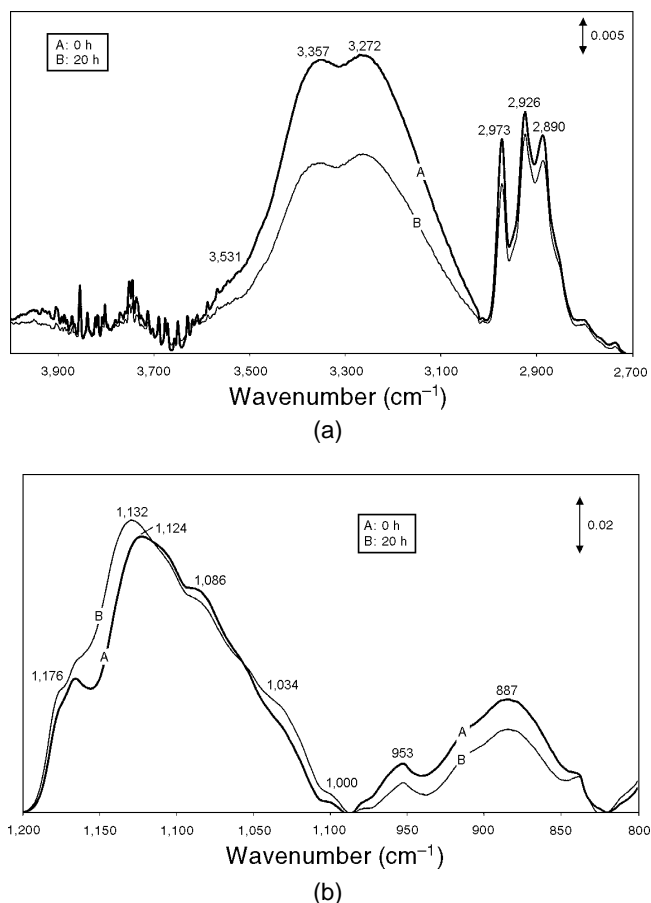


**FIGURE 14.** RAIR spectra of sulfane-treated Al 2024-T3 immersed in 0.5 M K<sub>2</sub>SO<sub>4</sub> solution at RT from 0 h to 20 h: (a) 4,000 cm<sup>-1</sup> to 2,700 cm<sup>-1</sup> and (b) 1,200 cm<sup>-1</sup> to 800 cm<sup>-1</sup>.

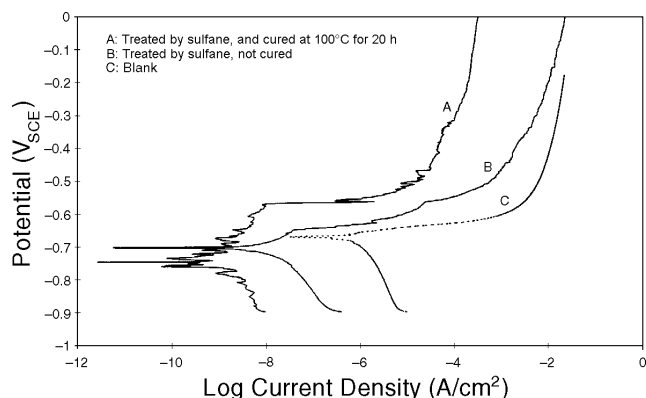


**FIGURE 15.** Potentiodynamic polarization curves of Al 2024-T3 in 0.5 M NaCl solution at pH 6.

air at RT for 336 h before exposure to SST for 360 h. The results (Table 2) show that the corrosion behavior of Al 2024-T3 treated by sulfane-silane and by chromate is comparable (i.e., only a few small pits were observed after testing). This demonstrates sulfane-silane treatment can be a promising replacement for chromating.

Although some important information concerning the evolution of the structure of a sulfane-silane film on Al 2024-T3 in different processes has been obtained from EIS study in a noncorrosive electrolyte like 0.5 M K<sub>2</sub>SO<sub>4</sub>, some unknown aspects remain, such as the structure and chemistry of the interfacial layer (unknown phase) between the silane film and metal oxide layer and its contribution to corrosion protection on metals. Thus, in the future work, the silane-metal interfacial region will be thoroughly analyzed using techniques such as RAIR and ToFSIMS depth profiling with a sulfur hexafluoride (SF<sub>6</sub>) primary source and spectra reconstruction. The behavior in the noncorrosive electrolyte will be compared with EIS in the corrosive electrolyte NaCl and with the performance of silane-coated metals in other corrosion tests.

## CONCLUSIONS

- ❖ Three effects were studied in EIS of BTESPT-treated Alloy Al 2024-T3 panels: the effect of continuous immersion time in 0.5 M K<sub>2</sub>SO<sub>4</sub> solution, the effect of curing time in air at 80°C prior to EIS analysis, and the effect of aging time at RT prior to EIS analysis. In all cases, the total impedance of the system increased markedly.
- ❖ The phase angle plot is more sensitive to the structural changes in the system than the impedance plot. An additional time constant, most likely indicative of a new phase between the silane film and the aluminum oxide, was observed in the phase angle plot in two of the three experiments.
- ❖ The significant increase of the total impedance of the system was attributed to the formation of siloxane structures -Si-O-Si- in the existing silane film by condensation of silanol groups -SiOH, generated from the hydrolysis of residual ester groups -SiOC<sub>2</sub>H<sub>5</sub> in the 0.5 M K<sub>2</sub>SO<sub>4</sub> electrolyte, and to the formation and growth of the unknown phase between the silane film and the Al<sub>2</sub>O<sub>3</sub> layer. The conclusion has been partly confirmed by RAIR surface analysis.
- ❖ Three successful equivalent circuits for the modeling of the observed changes in the EIS spectra vs time were presented. These circuits fit the data very well.
- ❖ EIS in a noncorrosive electrolyte has been demonstrated to be a useful tool for determining the conditions for depositing silane films on metals with optimum conditions for corrosion protection. A fully cross-linked sulfane-silane film with a higher impedance in its EIS spectrum showed excellent corrosion protection on Al 2024-T3 in the potentiodynamic polarization test and 360-h SST (ASTM B117).
- ❖ A fully cross-linked sulfane-silane film on Al 2024-T3 can be obtained either through curing the film at a higher temperature (e.g., 100°C for 4 h), and/or

**TABLE 2**  
Corrosion Evaluation of Al 2024-T3 Untreated,  
Treated by Sulfane-Silane and Chromate after 360 h of SST

Treatment	Rust Coverage on the Tested Surface (%)	Rust Mark
A1050 alkaline-cleaned	100	WR <sup>(A)</sup> 10
Chromated (Chromicoat 103 <sup>†</sup> )	A few pits on the surface	WR-spot
Sulfane-silane-treated (cured at 100°C for 10 min, and then aged in air at RT for 336 h)	A few pits on the surface	WR-spot

<sup>(A)</sup> White rust on the surface of the Al alloy.

through aging the film in humid air at RT for a longer time.

❖ The barrier properties of the unknown phase observed in EIS are possibly the origin of the high corrosion protection performance and will be the subject of further study.

## ACKNOWLEDGMENTS

The authors acknowledge the financial support provided by Brent International PLC in Bletchley, U.K. and the operation of SST by Chemetall Oakite Co. in Berkeley Heights, NJ.

## REFERENCES

- W.J. van Ooij, T.F. Child, *Chem. Tech.* 28 (1998): p. 26.
- V. Subramanian, W.J. van Ooij, *Corrosion* 54 (1998): p. 204.
- V. Subramanian, "Silane Coupling Agents for Corrosion Protection" (Ph.D. thesis Diss., University of Cincinnati, 1999).
- W.J. van Ooij, G. Prasad Sundararajan, D. Zhu, S.K. Jayaseelan, "Silane Coatings for Replacement of Phosphate Chromated Pretreatments of Automotive Metal Sheets," *Corros. Sci. Eng. (JCSE)* at <http://www.cp.umist.ac.uk/JCSE/vol2/paper14/v2p14.html>.
- G. Prasad Sundararajan, W.J. van Ooij, *Surf. Eng.* 16 (2000): p. 315.
- W.J. van Ooij, S.K. Jayaseelan, D. Zhu, G. Prasad Sundararajan, Y. Fu, *Proc. U.S. Navy and Industry Technology Information Exchange (Port Hueneme, Naval Surface Weapons Center, 1999)*, on CD.
- W.J. van Ooij, D. Zhu, G. Prasad, S.K. Jayaseelan, Y. Fu, N. Teredesai, *Surf. Eng.* 16 (2000): p. 386.
- E.P. Plueddemann, *Silane Coupling Agents*, 2nd ed. (New York, NY: Plenum Press, 1991).
- K.L. Mittal, ed., *Silanes and other Coupling Agents* (Utrecht, the Netherlands: VSP, 1992).
- H.-D. Luginsland, "Reactivity of the Sulfur Functions of the Disulfane Silane TESP and the Tetrasulfane Silane TESP," 155th Technical Meeting, held April 13-16, 1999, paper no. 74 (Chicago, IL: American Chemical Society, Rubber Division, 1999).
- R.F. Allen, N.C. Baldini, eds., *Annual Book of ASTM Standards*, (West Conshohocken, PA: ASTM, 1998), p. 188.
- F. Mansfeld, S. Lin, S. Kim, H. Shin, *J. Electrochem. Soc.* 137, (1990): p. 78.
- C. Chen, F. Mansfeld, *Corros. Sci.* 39 (1997): p. 1,075.
- F. Mansfeld, *J. Appl. Electrochem.* 25 (1995): p. 187.
- H. Shin, F. Mansfeld, *Corrosion* 45 (1989): p. 610.
- H. Xiao, F. Mansfeld, *J. Electrochem. Soc.* 41 (1994): p. 2,332.
- H.P. Hack, J.R. Scully, *J. Electrochem. Soc.* 138 (1991): p. 33.
- E.P.M. van Westing, G.M. Ferrari, J.H.W. de Wit, *Corros. Sci.* 36 (1994): p. 979.
- M.D.G. Destreti, J. Vogelsang, L. Fedrizzi, F. Deflorian, *Progr. Org. Coat.* 37 (1999), p. 69.
- Th. Van Schaftinghen, "Characterization of Silane Layers on Metallic Substrates" (M.S. thesis, Vrije Universiteit Brussel, 1999), p. 39.
- G. Prasad Sundararajan, "Silane-Base Pretreatments of Electrocoated Metals for Corrosion Protection" (M.S. thesis, University of Cincinnati, 2000), p. 130.
- S.K. Jayaseelan, "Silane Coupling Agents for Rubber-to-Metal Adhesion" (M.S. thesis, University of Cincinnati, 2000), p. 125.
- N.G. McCrum, B.E. Read, G. Williams, *Anelastic and Dielectric Effect in Polymeric Solids* (New York, NY: Dover Publications Inc., 1991).
- A.M. Beccaria, L. Chiaruttini, *Corros. Sci.* 41 (1999): p. 885.
- W.J. van Ooij, *Rubb. Chem. Technol.* 57 (1984): p. 421.
- J.R. MacDonald, ed., *Impedance Spectroscopy* (New York, NY: John Wiley & Sons, 1987).
- S.F. Mertens, C. Xhoffer, B.C. Cooman, E. Temmerman, *Corrosion* 53 (1993): p. 381.
- E.P.M. van Westing, G.M. Ferrari, J.H.W. de Wit, *Corros. Sci.* 34 (1993), p. 1,511.

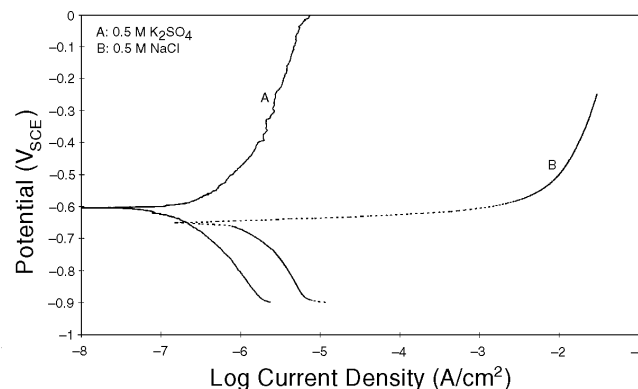


**FIGURE A-1.** Potentiodynamic polarization curves of Al 2024-T3 blank in 0.5 M  $K_2SO_4$  and 0.5 M NaCl solutions at pH 6.

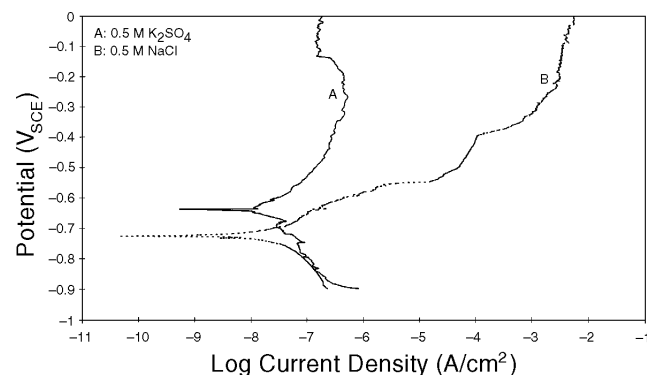


**FIGURE A-2.** Potentiodynamic polarization curves of sulfane-treated Al 2024-T3 in 0.5 M  $K_2SO_4$  and 0.5 M NaCl solutions at pH 6.

**TABLE B1**  
Summary of Fitted EIS Data for the Immersion Process<sup>(A)</sup>

t (h)	$Q_{sil} \pm dQ_{sil}$ ( $\Omega$ )	$n_{sil} \pm dn_{sil}$	$R_{sil} \pm dR_{sil}$ ( $\Omega$ )	$C_{sil} \pm dC_{sil}$ (F)
<b>Silane Film</b>				
0.16	$3.23E + 06 \pm 1.91E + 05$	$9.16E - 01 \pm 5.76E - 03$	$1.85E + 03 \pm 5.58E - 01$	$1.30E - 07 \pm 8.99E - 11$
2	$5.47E + 06 \pm 6.05E + 05$	$9.48E - 01 \pm 9.69E - 03$	$1.88E + 04 \pm 9.24E + 03$	$1.08E - 07 \pm 8.08E - 08$
4	$6.69E + 06 \pm 5.70E + 05$	$9.54E - 01 \pm 7.96E - 03$	$2.76E + 04 \pm 1.04E + 04$	$9.83E - 08 \pm 1.61E - 09$
8	$7.97E + 06 \pm 7.50E + 04$	$9.66E - 01^{(B)} \pm 0.00E - 00$	$1.04E + 05 \pm 2.38E + 04$	$9.44E - 08 \pm 2.21E - 09$
t (h)	$Q_{un} \pm dQ_{un}$ ( $\Omega$ )	$n_{un} \pm dn_{un}$	$R_{un} \pm dR_{un}$ ( $\Omega$ )	$C_{un} \pm dC_{un}$ (F)
<b>Unknown Phase</b>				
0.16	N/A	N/A	N/A	N/A
2	$2.09E + 06 \pm 1.60E + 06$	$7.50E - 01 \pm 2.05E - 01$	$1.85E + 04 \pm 9.96E + 03$	$8.08E - 08 \pm 5.05E - 08$
4	$6.77E + 06 \pm 1.34E + 06$	$7.69E - 01 \pm 4.48E - 02$	$1.88E + 05 \pm 1.27E + 04$	$4.79E - 08 \pm 1.80E - 09$
8	$1.39E + 07 \pm 2.35E + 06$	$8.57E - 01 \pm 5.15E - 02$	$4.75E + 05 \pm 2.65E + 04$	$3.71E - 08 \pm 8.88E - 10$
t (h)	$Q_{ox} \pm dQ_{ox}$ ( $\Omega$ )	$n_{ox} \pm dn_{ox}$	$R_o \pm dR_o$ ( $\Omega$ )	
<b>Oxide Film</b>				
0.16	$6.37E + 04 \pm 5.15E + 02$	$8.73E - 01 \pm 3.24E - 03$	$3.99E + 01 \pm 8.24E + 01$	
2	$7.99E + 04 \pm 2.66E + 03$	$8.52E - 01 \pm 2.33E - 03$	$4.27E + 01 \pm 1.16E - 01$	
4	$9.07E + 04 \pm 2.24E + 02$	$8.54E - 01 \pm 3.41E - 03$	$4.08E + 01 \pm 1.10E - 01$	
8	$9.42E + 04 \pm 2.36E + 03$	$8.61E - 01^{(B)} \pm 0.00E - 00$	$4.10E + 01 \pm 9.35E - 01$	

<sup>(A)</sup> t = time, Q = CPE parameter ( $=1/Y_0$ ), and F = Farad (unit of capacitance).

<sup>(B)</sup> The parameters were fixed after the 1st iteration, by which the fit was improved slightly.

**TABLE B2**  
Summary of Fitted EIS Data for the Curing Process<sup>(A)</sup>

t (h)	$Q_{sil} \pm dQ_{sil}$ ( $\Omega$ )	$n_{sil} \pm dn_{sil}$	$R_{sil} \pm dR_{sil}$ ( $\Omega$ )	$C_{sil} \pm dC_{sil}$ (F)
<b>Silane Film</b>				
0.16	$2.17E + 06 \pm 3.27E + 05$	$8.91E - 01 \pm 1.39E - 02$	$3.69E + 03 \pm 7.23E + 00$	$1.40E - 07 \pm 1.11E - 10$
1	$5.46E + 06 \pm 2.95E + 05$	$9.47E - 01 \pm 5.43E - 03$	$6.53E + 03 \pm 1.01E + 02$	$1.08E - 07 \pm 1.35E - 10$
2	$8.39E + 06 \pm 7.30E + 05$	$9.83E - 01 \pm 8.40E - 03$	$4.61E + 03 \pm 1.94E + 04$	$1.03E - 07 \pm 3.03E - 09$
3.3	$1.04E + 07 \pm 8.00E + 05$	$9.77E - 01 \pm 7.42E - 03$	$1.35E + 05 \pm 8.63E + 04$	$8.25E - 08 \pm 1.33E - 09$
5.3	$8.75E + 06 \pm 1.07E + 05$	$9.71E - 01 \pm 0.00E + 00$	$2.12E + 05 \pm 9.22E + 04$	$9.54E - 08 \pm 1.10E - 09$
6	$1.14E + 07 \pm 2.89E + 05$	$9.79E - 01 \pm 2.95E - 03$	$8.73E + 05 \pm 0.00E + 00$	$7.73E - 08 \pm 3.70E - 10$
t (h)	$Q_{un} \pm dQ_{un}$ ( $\Omega$ )	$n_{un} \pm dn_{un}$	$R_{un} \pm dR_{un}$ ( $\Omega$ )	$C_{un} \pm dC_{un}$ (F)
<b>Unknown Phase</b>				
0.16	N/A	N/A	N/A	N/A
1	N/A	N/A	N/A	N/A
2	$6.23E + 06 \pm 1.17E + 06$	$7.73E - 01 \pm 5.13E - 02$	$4.22E + 05 \pm 3.09E + 04$	$5.15E - 08 \pm 2.87E - 09$
3.3	$2.14E + 07 \pm 4.47E + 06$	$8.06E - 01 \pm 4.44E - 02$	$3.61E + 06 \pm 1.84E + 05$	$2.19E - 08 \pm 1.03E - 09$
5.3	$3.48E + 07 \pm 5.35E + 06$	$8.77E - 01 \pm 5.15E - 02$	$7.45E + 06 \pm 3.79E + 05$	$1.89E - 08 \pm 3.97E - 10$
6	$4.17E + 07 \pm 4.89E + 06$	$8.99E - 01 \pm 0.00E + 00$	$2.62E + 07 \pm 4.61E + 05$	$1.90E - 08 \pm 2.23E - 09$
t (h)	$Q_{ox} \pm dQ_{ox}$ ( $\Omega$ )	$n_{ox} \pm dn_{ox}$	$R_o \pm dR_o$ ( $\Omega$ )	
<b>Oxide Film</b>				
0.16	$4.74E + 04 \pm 5.23E + 02$	$8.82E - 01 \pm 3.56E - 03$	$3.67E + 01 \pm 1.15E - 01$	
1	$7.58E + 04 \pm 8.13E + 02$	$8.28E - 01 \pm 4.77E - 03$	$3.95E + 01 \pm 1.01E - 00$	
2	$1.24E + 05 \pm 7.11E + 03$	$7.65E - 01 \pm 2.00E - 02$	$4.12E + 01 \pm 1.26E - 00$	
3.3	$2.49E + 05 \pm 3.09E + 04$	$7.36E - 01 \pm 3.80E - 02$	$4.32E + 01 \pm 1.42E - 00$	
5.3	$4.15E + 05 \pm 1.11E + 05$	$6.57E - 01 \pm 6.39E - 02$	$4.32E + 01 \pm 1.22E - 01$	
6	N/A	N/A	$4.17E + 01 \pm 1.16E - 00$	

<sup>(A)</sup> t = time, Q = CPE parameter ( $=1/Y_0$ ), and F = Farad (unit of capacitance).

**TABLE B3**  
Summary of Fitted EIS Data for the Aging Process<sup>(A)</sup>

t (h)	$Q_{\text{sil}} \pm dQ_{\text{sil}}$ ( $\Omega$ )	$n_{\text{sil}} \pm dn_{\text{sil}}$	$R_{\text{sil}} \pm dR_{\text{sil}}$ ( $\Omega$ )	$C_{\text{sil}} \pm dC_{\text{sil}}$ (F)
<b>Silane Film</b>				
24	$2.99\text{E} + 06 \pm 2.61\text{E} + 05$	$8.93\text{E} - 01 \pm 8.10\text{E} - 03$	$6.98\text{E} + 02 \pm 8.40\text{E} + 00$	$1.97\text{E} - 07 \pm 9.58\text{E} - 09$
72	$5.74\text{E} + 06 \pm 0.00\text{E} + 00^{(B)}$	$9.30\text{E} - 01^{(B)} \pm 0.00\text{E} + 00$	$1.42\text{E} + 04 \pm 6.54\text{E} + 02$	$1.25\text{E} - 07 \pm 0.00\text{E} + 00$
96	$6.33\text{E} + 06^{(B)} \pm 0.00\text{E} + 00$	$9.56\text{E} - 01^{(B)} \pm 0.00\text{E} + 00$	$2.74\text{E} + 04 \pm 2.43\text{E} + 02$	$1.28\text{E} - 07 \pm 0.00\text{E} + 00$
120	$7.10\text{E} + 06 \pm 1.69\text{E} + 05$	$9.60\text{E} - 01 \pm 2.61\text{E} - 03$	$6.28\text{E} + 04 \pm 1.90\text{E} + 02$	$1.16\text{E} - 07 \pm 1.35\text{E} - 09$
t (h)	$Q_{\text{ox}} \pm dQ_{\text{ox}}$ ( $\Omega$ )	$n_{\text{ox}} \pm dn_{\text{ox}}$	$R_{\text{o}} \pm dR_{\text{o}}$ ( $\Omega$ )	
<b>Oxide Film</b>				
24	$5.24\text{E} + 04 \pm 4.01\text{E} + 02$	$9.16\text{E} - 01 \pm 2.74\text{E} - 03$	$3.70\text{E} + 01 \pm 9.79\text{E} - 01$	
72	$6.45\text{E} + 04 \pm 6.54\text{E} + 02$	$8.99\text{E} - 01^{(B)} \pm 0.00\text{E} + 00$	$3.71\text{E} + 01 \pm 0.00\text{E} + 00$	
96	$6.53\text{E} + 04 \pm 7.24\text{E} + 02$	$9.09\text{E} - 01^{(B)} \pm 0.00\text{E} + 00$	$4.14\text{E} + 01 \pm 7.14\text{E} - 01$	
120	$6.81\text{E} + 04 \pm 9.76\text{E} + 02$	$8.97\text{E} - 01 \pm 6.60\text{E} - 03$	$4.06\text{E} + 01 \pm 8.06\text{E} - 01$	

<sup>(A)</sup> t = time, Q = CPE parameter ( $=1/Y_0$ ), and F = Farad (unit of capacitance).

<sup>(B)</sup> The parameters were fixed after the 1st iteration, by which the fit was improved slightly.

29. G. Socrates, *Infrared Characteristic Group Frequencies* (New York, NY: John Wiley & Sons, 1994), p. 188.  
30. M.W. Urban, *Vibrational Spectroscopy of Molecules and Macromolecules on Surfaces* (New York, NY: John Wiley & Sons, 1993), p. 305.

## APPENDIX A

### Comparison of Corrosivity of $K_2SO_4$ and NaCl

Potentiodynamic polarization tests were done on Al 2024-T3 untreated and treated by sulfane-silane, respectively, in both 0.5 M  $K_2SO_4$  and 0.5 M NaCl solutions at pH 6. The purpose of the tests was to evaluate the corrosivity of  $K_2SO_4$  and NaCl solutions. Before the data was recorded, the tested specimens were immersed in the electrolytes for 40 min in an attempt to achieve a steady state. The results are presented in Figures A-1 and A-2. It is evident from Figure A-1 that both cathodic and anodic currents reduced significantly in 0.5 M  $K_2SO_4$  for Al 2024-T3 blank, compared with the case of 0.5 M NaCl. In the case of sulfane-treated Al 2024-T3 (Figure A-2), although there was no difference between cathodic currents in 0.5 M  $K_2SO_4$  and 0.5 M NaCl solutions, the anodic reaction (or metal dissolution) was apparently inhibited in 0.5 M  $K_2SO_4$ . Based on the comparisons above, 0.5 M  $K_2SO_4$  was thus chosen as the noncorrosive electrolyte in the current EIS study.

**TABLE B4**  
Dielectric Constants  $\epsilon$   
of Sulfane-Silane Film in the Curing Process at 80°

t (h)	$\epsilon$
0.16	15.85
1	12.22
2	11.66
3.3	9.34
5.3	10.80
6	8.75

## APPENDIX B

Fitted EIS data for the Bis-Sulfane treated Al 2024-T3 systems studied in this paper.

The values of capacitance in Tables B1 to B4 were calculated from the CPE parameters,  $Y_0$  ( $=1/Q$ ) and n, using Equation (6). The errors in capacitance were obtained using the error propagation method applied to Equation (6).<sup>26</sup>

It should be noted that the fitted EIS data for the  $Al_2O_3$  film could not be determined in some cases because of instrumental limitations ( $10^{-3}$  Hz). The time constant for the  $Al_2O_3$  film was located at low frequencies, and in most cases a complete time constant for the  $Al_2O_3$  film could not be obtained.